A new vacuum membrane distillation system using an aspirator: concept modeling and optimization

Mohamed I. Hassan[a], Ayoola T. Brimmo[a], Jaichander Swaminathan[b], John H. Lienhard V[b], Hassan A. Arafat[a],*

[a]*Institute Center for Water and Environment (iWATER), Masdar Institute of Science and Technology, Abu Dhabi, United Arab Emirates, P.O. Box 54224, Abu Dhabi, UAE, Tel. +971 52 9192514; email: miali@masdar.ac.ae (M.I. Hassan), Tel. +971 509042782; email: abrimmo@masdar.ac.ae (A.T. Brimmo), Tel. +971 2 810 9119; email: harafat@masdar.ac.ae (H.A. Arafat)*
[b]*Department of Mechanical Engineering, Massachusetts Institute of Technology, 77 Massachusetts Avenue, Cambridge, MA 02139 4307, USA, Tel. +1 6177154046; email: jaichu@mit.edu (J. Swaminathan), Tel. +1 6172531000; email: lienhard@mit.edu (J.H. Lienhard V)*

ABSTRACT

The aim of this study is to validate and optimize a new concept of implementing an aspirator as the vacuum generator for a vacuum membrane distillation (VMD) setup. Numerical models are developed for the aspirator, and its interconnectivity with the VMD chamber is demonstrated. A correlation to estimate the minimum aspirator pump size for a given permeate mass flow is deduced from these models. The dependence of the system's specific power consumption (per unit permeate flow) on the feed flow rate, number of membrane sheets in the VMD module, and vacuum pressure is investigated. The gained output ratio (GOR) of the proposed system is comparable (GOR ≈ 0.8) to conventional single-stage VMD with a vacuum pump, if brine heat is recovered using a regenerator to preheat the incoming feed. The theoretical power requirement for a vacuum pump is lower than that used by the aspirator system, if all vapor is condensed and only non-condensable gasses are removed by the vacuum pump. At lower vapor pressures, when complete condensation is difficult, the vacuum pump power consumption is comparable to that of the aspirator system if about 60% of the vapor produced reaches the vacuum pump.

Keywords: Membrane distillation; Aspirator; Vacuum membrane distillation; GOR; Energy consumption

1. Introduction

Membrane distillation (MD) is a thermally driven process in which vapor is transferred through the non-wetted pores of a hydrophobic membrane, with the driving force being a vapor pressure difference between the two sides of the membrane pores, which often results from a temperature difference between the two sides. MD can potentially be used for various applications, most notably in desalination [1]. It can also be used for environmental clean-up (removal of volatile organic chemicals from water) and in food and medical applications [2]. In the literature, there are four different MD configurations most commonly applied [1]. These are: (1) direct contact membrane

*Corresponding author.

distillation (DCMD); (2) sweeping gas membrane distillation (SGMD); (3) vacuum membrane distillation (VMD); and (4) air gap membrane distillation (AGMD).

The MD process has several advantages, compared to other membrane-based desalination processes, such as reverse osmosis (RO). These advantages include MD's fitness for intermittent energy supply and ability to use low-grade heat [3–6]. At present, water desalination using the MD process, including using the VMD configuration, is still mainly in the research and pilot testing phase. Several studies have been conducted on this process worldwide, but it has not been adopted for utility-scale commercial application yet [7]. The primary reason for the limited commercialization is the high cost of water produced using MD, especially if no free source of thermal energy is available, which makes it difficult for MD to compete with other desalination processes, such as RO [8]. New designs and process improvements will eventually lead to cost reductions that will make the MD process commercially viable for specific applications.

VMD is among the most promising MD configurations as the additional driving force due to the vacuum on the permeate side leads to a higher flux. In VMD, a pressure below the saturation pressure corresponding to the feed temperature needs to be maintained in the permeate chamber. Higher feed temperature or lower vacuum pressure both lead to an increase in distillate production. One concern with VMD systems is their increased potential for membrane wetting, as the vacuum generated in the permeate side may lead to a transmembrane pressure exceeding the liquid entry pressure of the membrane. Thus, the vacuum level needs to be controlled carefully. In the VMD systems reported in the literature, a vacuum pump is used to draw the vapor out of the permeate chamber. The permeate stream is then passed through a condenser to condense and recover the vapor [9]. A post-condenser moisture trap is usually used to protect the vacuum pump. There are several challenges with this design. These include:

(1) The power cost for the vacuum pump during operation depends on the extent of condensation in the condenser. At lower pressures, complete condensation is difficult and hence vacuum pumping power will be high.
(2) The recovery of water in this setup is done by condensing the vapor, using a heat exchanger. The cost of running a coolant in the exchanger adds to the cost of the fresh water produced.
(3) Incomplete recovery of vapor leads to vapor penetrating the vacuum pump. Vacuum pumps need to be sealed and lubricated. Both the seals and lubricant are negatively affected
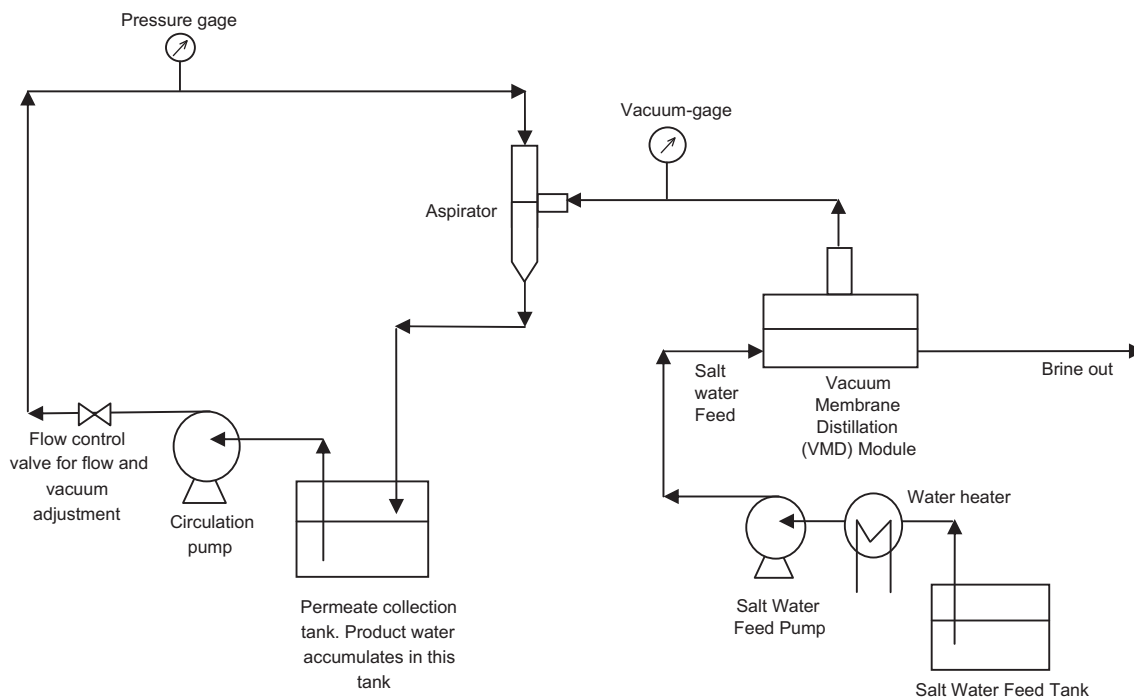

Fig. 1. The new VMD design.

by the presence of water vapor in the pump. Despite the use of moisture traps or demisters to protect the pump, minute amounts of vapor will inevitably damage the vacuum pump in the long run.

(4) Finally, typical vacuum pumps are not designed to operate continuously over extended periods of time, as would be needed in a plant-scale VMD system. Rather, they are operated intermittently.

In this work, a new design concept to mitigate the above risks associated with vacuum pumps in VMD systems is introduced: an aspirator is used to create the vacuum and simultaneously condense the vapor into the aspirator's circulating liquid, thus eliminating the need for the vacuum pump, the moisture trap, and the condenser, while ensuring full recovery of all vapor produced. A schematic diagram of the design is shown in Fig. 1. The aspirator, a simple device with no moving parts, is described in detail in Section 2. This new design has the potential to enable cost reduction of the VMD process and easier control of the vacuum level by controlling the flow rate of liquid through the aspirator.

This system can be used in the case of desalination by VMD, where the circulated liquid used to create the vacuum in the aspirator (water) is the same substance as the vapor permeating through the membrane. Using this design for VMD desalination, the aspirator creates vacuum in the permeate side of the membrane module. As water vapor comes in contact with the aspirator liquid (which is also water), the vapor condenses into the circulating water. The purified water is then accumulated in the permeate collection tank and can be recovered from there. Non-condensable gasses (e.g. air) will bleed out of the permeate collection tank.

The goal of this study is to validate this new concept and to optimize the design parameters, as a precursor step for future prototype construction and testing. It is worth mentioning that, while Venturi ejectors using steam (also a form of an aspirator) have long been used for multi-effect desalination (MED), in the present work, to our best knowledge, for the first time an aspirator has been used in a membrane desalination system for simultaneous vacuum generation and product vapor recovery.

2. Methodology

The aspirator is a device that generates reduced pressure in a contraction section due high flow velocity, following Bernoulli's principle. Typical aspirators have a Venturi shape—a converging–diverging nozzle—as shown in Fig. 2(a). These systems' energy consumption is that required to force a flow through the contracting section. The aspirator-generated vacuum pressure then provides a passive alternative to a mechanical vacuum pump in a VMD system.

The aspirator modeled in this study was designed based on the ISO 5167 standards [10] for sizing a Venturi with the following key considerations (see Fig. 2(a)):

(1) Entrance and exit cylinders (section A and E respectively) length (L) equal to entrance cylinder diameter (d_1);
(2) The angle/overall length of convergent section (section B) of 21° and $2.7(d_1 - d_2)$, respectively, where d_2 is the throat's (section C) diameter;
(3) Throat length (l) of $d \pm 0.03d$;
(4) Conical divergent section (section D) making an angle of 7° with the horizontal.
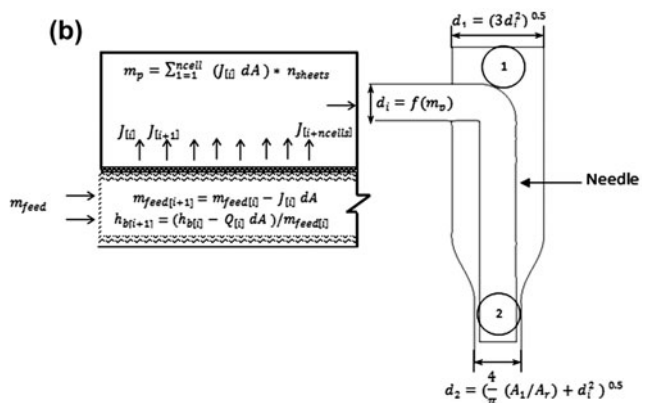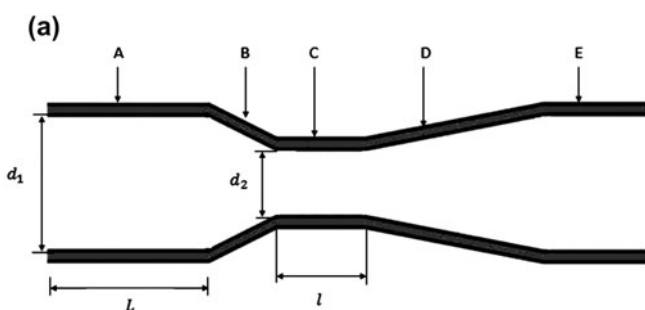

Fig. 2. Schematic diagrams of: (a) the aspirator; and (b) system parameters connecting VMD to aspirator.

Vacuum pressure is generated in the aspirator by running pure water through the aspirator's throat, using a water pump. The pure water flow rate and inlet pressure determine the vacuum pressure in the throat section, according to the Bernoulli equation (below), and the inlet/throat area ratio, according the continuity equation (below). In typical aspirator designs, the vacuum pressure is usually tapped from the throat's external walls. However, for improved permeate flow from the VMD, we require the largest possible piping diameter (d_i) to connect the aspirator to the desalination unit. From a geometric perspective, the exterior throat surface limits the size of the permeate pipe, hence we propose the "injector needle" with adiabatic walls for connecting the aspirator to the membrane chamber (Fig. 2(b)). The permeate stream will condense into the aspirator's pure water stream and can be removed from the collection tank.

In a vacuum system, by analogy to electrical current, one can get a gaseous flow through the piping which offers a certain resistance, known as impedance. The reciprocal of the impendence (resistance to the gaseous flow) is the pipe's conductance [11]. Aspirator sizing is dependent on the level of vacuum required and the piping's conductance (which is directly linked to the expected permeate mass flow from the MD module). Also, when water is used as the working fluid, the strength of the vacuum produced by the aspirator is limited by the vapor pressure of the water (which is 3.2 kPa at 25°C). Its dependence on the level of vacuum can be estimated directly via Bernoulli's principle; however, the vacuum impendence also affects the vacuum conductance for a given pipe diameter. The conductance limits the flow in the system, hence constituting an important parameter in sizing the aspirator for the VMD system. Fig. 2(b) is a schematic diagram of the integrated VMD/aspirator system. Our objective is to maximize the needle conducted permeate flow due to the throat's developed vacuum.

Using this approach, the needle's diameter can be maximized, as it can go as high as 90% of the throat's diameter. Using the Engineering Equation Solver (EES) software—a simultaneous equation solver which uses a Newton iteration method to converge on the solution—equations governing the workings of the aspirator and the VMD system are simultaneously solved in order to validate and optimize the proposed concept. The analytical EES model for MD previously developed and published by the authors [12] was modified for this purpose. More details about the EES code can be found in [12]. The feed water (to MD module) temperature was assumed to be 85°C, the feed flow channel width was assumed to be 4 mm, and the module width to be 0.7 m. In all modeled

systems, the membrane length was assumed to be 10 m. The assumed membrane's porosity, pore diameter, thickness, thermal conductivity, flow channel depth, and module width are 0.8, 0.2 μm, 0.2 mm, 1.2 W/m-K, 4 mm, and 0.7 m, respectively. These values of design parameters were based on our previous modeling work and were found to yield the optimum cost value for a single-stage MD system [13]. Computational fluid dynamics (CFD) are adapted for estimating the aspirator's conductance and monitor its cavitation behavior, using the commercial code, StarCCM+ [14].

The parameters considered for the optimization study are the aspirator contraction area ratio, A_r, the VMD feed flow, m_{feed}, number of membrane sheets in the module, n_{sheets}, and the target vacuum pressure. The membrane sheets are units of the membrane arranged in parallel, in a plate and frame modular arrangement for example, to increase the membrane area and subsequently the production rate of the MD plant. As suggested by Ali et al. [13], a uniform feed of m_{feed} of 3 kg/s and a target vacuum pressure of 17 kPa is considered for the contraction area ratio optimization study. About 1 kPa is lost in the production pipes and in the membrane chamber. The 17 kPa was chosen as a practical value for VMD permeate vapor. The saturation temperature at 17 kPa is 56.6°C; factoring in the additional possible pressure drop due to the membrane resistance, the temperature of the feed should be kept above the 60°C. Lower vacuum pressures will lead to even lower feed temperatures, which will then carry a penalty of lower flux rate due to the low feed temperature.

The m_{feed} and n_{sheets} variables are somewhat entangled. Hence, at first, we investigate the effect of increasing m_{feed} for different n_{sheets} values using an aspirator with $A_r = 0.1$. Based on the total specific power, which equals the power to the MD feed pump ($Power_{feed}$) plus the power to the aspirator pump ($Power_{asp}$), we estimate the optimum m_{feed} values for each n_{sheets}. It is important to note that the specific power is calculated per unit of product, not feed water. Using the estimated optimum m_{feed} values, we investigate the optimum n_{sheets} value for our system. A target vacuum pressure of 17 kPa was also utilized in optimizing these variables. However, applying an identical approach, the target vacuum pressure was changed to 55 kPa to investigate the effect of vacuum pressure on system performance.

The aspirator's governing equations are the conservation of energy principle, as described by the Bernoulli equation (Eq. (1)), and conservation of mass (Eq. (2)). The Bernoulli equation, including corrections for discharge coefficients, is

$$P_1 + \frac{1}{2C_d} \rho_{fresh} v_1^2 + \rho g z_1 = P_2 + \frac{1}{2C_d} \rho_{fresh} v_2^2 + \rho g z_2, \qquad (1)$$

where P is the pressure at position 1 and 2 inlet, C_d is the discharge coefficient taking into account the losses due to friction, ρ_{fresh} is the aspirator fluid's density, v is the fluid's velocity, g is the gravitation constant, z is the elevation of the fluid above a reference position, and subscripts 1 and 2 refer to the Venturi's inlet and throat positions, respectively (see Fig. 2(b)). In this equation, P_1 is based on specification from the applied water and P_2 is the desired membrane pressure (i.e. vacuum level), per the specifications of the VMD unit. In this case, P_1 is 200 kPa and P_2 is 17 or 55 kPa. v_1 and v_2 are correlated via the mass conservation equation:

$$m_{fresh} = \rho_{fresh} v_1 A_1 = \rho_{fresh} v_2 A_2, \qquad (2)$$

where m_{fresh}, is the mass flow rate through the aspirator and A is the cross-sectional area perpendicular to the velocity stream vector. In our aspirator design,

$$A_1 = \pi d_1^2 / 4 \qquad (3)$$

$$A_2 = \pi(d_2^2 - d_i^2)/4 \qquad (4)$$

d_i is the diameter of the aspirator's connecting pipe (needle) which depends on the desired conductance; a parameter which portrays the amount of permeate fluid flow the pump can draw at a certain vacuum pressure. This is an important factor in quantifying the pump's flow capacity. However, piping conductance available in the literature is estimated for straight connecting pipes with air as the "sucked" fluid [15]. The literature values for the conductance of the L-shaped profile of our connecting pipe were not found; hence we developed a CFD model to estimate this parameter as a function of the pipe's diameter. In this model, the segregated flow model was adapted in solving the Navier–Stokes equations with the linkage between the momentum and continuity equations achieved with a predictor–corrector approach. The k-epsilon two-layer turbulence model was adapted to model the turbulent conditions. The interaction of the gaseous (steam) and liquid (water) phases in the system is modeled using the multi-phase segregated approach where conservation equations are solved for each phase and the cavitation interaction between each phase modeled based on the Rayleigh–Plesset equation [16,17]. Based on our mesh sensitivity

analysis, a 2.5 mm grid base size was adapted for the CFD model analysis.

Varying d_i, the maximum expected vapor permeate mass flow (i.e. conductance), m_p, through the pipe is estimated to obtain a relation for d_i as a function of m_p:

$$d_i = f(m_p) \qquad (5)$$

where m_p is in kg/s. d_2 is estimated using Eqs. (4) and (6) based on a predefined aspirator's contraction ratio, A_r,

$$A_r = A_2 / A_1 \qquad (6)$$

and an estimation of d_1 to ensure the needle area is at most one-third the aspirator's flow inlet area in order to minimize the pressure drop in that section.

The pump power, $Power_{asp}$, in the aspirator loop per unit volume of water produced (specific pump power) is estimated using the equation:

$$Power_{asp} = (P_2 - P_1) \times m_{fresh}/(\rho_{fresh} \times \epsilon_p \times vol_p), \qquad (7)$$

where ϵ_p is the pump's efficiency and vol_p is the volume flow rate of water pumped. In Eqs. (4)–(7), the variable m_p is required to estimate vol_p and d_i. However, this variable is dependent on the VMD parameter. This necessitates the introduction of the membrane desalination unit's governing equations.

In a VMD process, the mass transfer phenomenon is coupled with heat transfer mechanisms. The heat transfer by conduction from the membrane surface to the bulk phase and the latent heat transfer accompanying the membrane vapor flux are the system's driving force for mass flow [18–20]. This can be visualized by spelling out the heat transfer equations governing these phenomena as suggested by Summers et al. [12]. From the conservation of energy equation, heat transfer by conduction from the bulk flow to the membrane is estimated as:

$$Q = h_w(T_b - T_m) \qquad (8)$$

where T_b and T_m are the bulk fluid and membrane temperatures, respectively, and h_w is the heat transfer coefficient estimated from the Nusselt number (Nu) correlation proposed by Gnielinski [21]:

$$Nu = \frac{\left(\frac{f}{8}\right)(Re - 1,000)Pr}{1 + 12.7\left(\frac{f}{8}\right)^{\frac{1}{2}}(Pr^{\frac{2}{3}} - 1)} \qquad (9)$$

where f is the smooth-wall friction factor, Re is the flow's Reynolds number, and Pr is the fluid's Prandtl number. From the definition of Nusselt number:

$$h_w = Nu \times k/d \tag{10}$$

where k is the fluid's thermal conductivity and d is the hydraulic diameter of the membrane's channel, estimated as:

$$d = 4A_c/P \tag{11}$$

where A_c and P are the flow cross-sectional area and wetted perimeter, respectively. From Eq. (8), T_b can be measured while T_m cannot due to the presence of the feed boundary layer. To estimate T_m, the conservation of energy is applied to equate the latent heat transfer across the membrane to the heat transfer by conduction as presented in Eq. (8). The latent heat transfer can be estimated by:

$$Q = J(h_{pm} - h_b) \tag{12}$$

where h_{pm} is the specific enthalpy of vapor at the permeate side, h_b is the specific enthalpy of the bulk feed water, and J is the mass flux through the membrane. J is estimated from the pressure difference across the membrane and the membrane's diffusion coefficient. As J is also dependent on T_m, Eqs. (8) and (12) have to be solved simultaneously. It is worth noting that the fluid's thermodynamic properties change along the direction of flow. Therefore, segmenting the membrane along this direction provides a more accurate approach. In doing so, a set of equations have to be introduced to preserve the principles of conservation:

$$m_{feed[i+1]} = m_{feed[i]} - J_{[i]}dA \tag{13}$$

$$h_{b[i+1]} = (h_{b[i]} - Q_{[i]}dA)/m_{feed[i]}, \tag{14}$$

where the subscript $[i]$ denotes the segment number, dA is the segment area, and m_{feed} is the mass flow of the feed water. The specific power requirement of the feed water pump is estimated by:

$$power_{feed} = m_{feed}(dp_{piping} + dp_{membrane\,channel})/(\rho_{feed} \times \epsilon_p \times vol_p) \tag{15}$$

The total specific pump power per volume of permeate produced is the summation of the feed pump and aspirator pump's specific pump power:

$$Power_{total} = Power_{feed} + Power_{asp} \tag{16}$$

The total mass flux through the membrane is then estimated by summing the mass fluxes through each segment:

$$m_p = \sum_{1=1}^{cell\ number} (J_{[i]}dA) \times n_{sheets} \tag{17}$$

In order to operate the system at the minimum possible specific power, the set of equations governing the aspirator, membrane, and auxiliary equipment operations are solved simultaneously with the aspirator's contraction ratio (A_r), feed flow into the membrane channel (m_{feed}) and number of membrane sheets (n_{sheets}) as variables. Upon coupling the system with these equations, the specific power requirement of the aspirators and feed flow pumps are estimated. A schematic diagram showing how all these equations come together to solve for the overall VMD–aspirator parameters is shown in Fig. 2(b).

3. Results and discussion

3.1. System visualization

Fig. 3 shows the water-phase volume fraction of the fluid inside the aspirator system. As expected, the figure shows water vapor flowing from the membrane chamber which condenses upon contact with liquid water flowing through the aspirator. However, the presence of water vapor on the walls of the throat must be noted, as this is due to the flashing of water when a sudden drop in pressure occurs. This can be mitigated by increasing the contraction ratio of the aspirator $(d_2 - d_i)/d_1$.

Fig. 4 presents the pipe's calculated conductance as a function of its diameter. By curve fitting the data, a relation which describes the adequate piping diameter for the expected conductance was found to be $d_i = 0.2115\, m_p^{0.4185}$.

3.2. Effects of system design parameters

3.2.1. Aspirator contraction ratio (A_r)

Varying A_r, the aspirator loop pump's power consumption is estimated as presented in Fig. 5. From the figure, an increase in the contraction ratio increases
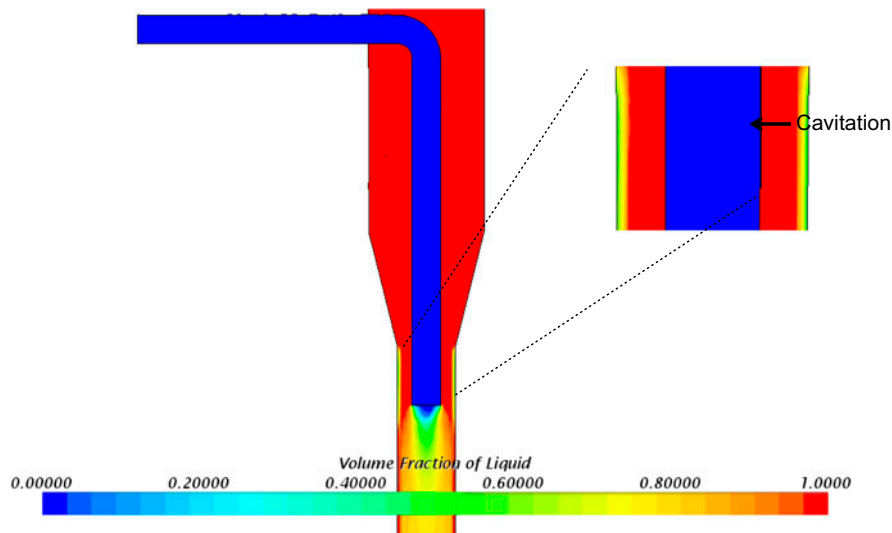
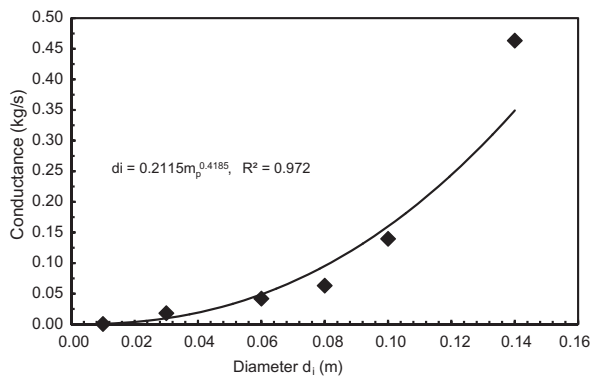Fig. 3. Water-phase volume fraction of the aspirator flow.

Fig. 4. MD–aspirator connecting pipe's conductance as a function of its diameter.
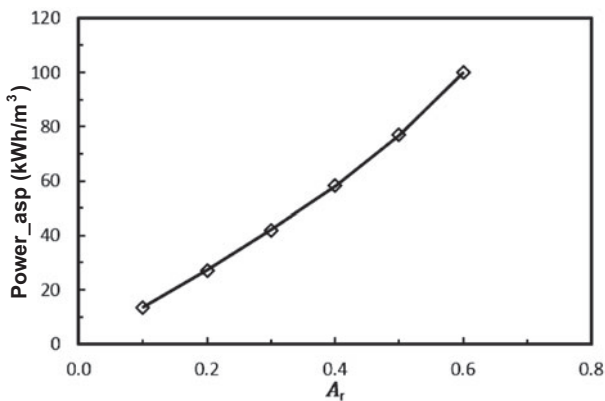

Fig. 5. Influence of aspirator's contraction ratio on power consumption of the aspirator loop pump.

the aspirator's specific pump power required to attain the target vacuum pressure. This is expected, based on Bernoulli's equation, because a larger annulus area would require more mass flow to attain a given pressure drop. This increase in mass flow in turn increases the pumping power. Furthermore, CFD analyses (Fig. 6) show that having a large A_r could give rise to instabilities in the aspiration in the form of a pre-throat pressure drop. The smaller A_r proved to be a better choice in this regard. However, as discussed earlier, there is a higher possibility of experiencing cavitation and noise at low values of A_r.

3.2.2. VMD feed flow rate and number of membrane sheets

Fig. 7(A) shows the specific pump power variation with m_{feed} for a single-membrane MD module. From this figure, it can be observed that as m_{feed} increases, the VMD feed water pump's specific power increases while the aspirator's specific pump power decreases. As the specific pump power is determined both by the total pumping power and the permeate flow rate, this trend yields a higher rate of increment in the total pump power of the feed water pump than the resulting permeate volumetric flow rate. The inverse of this is experienced in the aspirator's pump. As a consequence, the total specific pumping power decreases initially, reaches a minimum and then steadily increases. To optimize the system, the minimum total specific pump power is our target. Thus, m_{feed} at the inflection point is recorded as the optimum value.
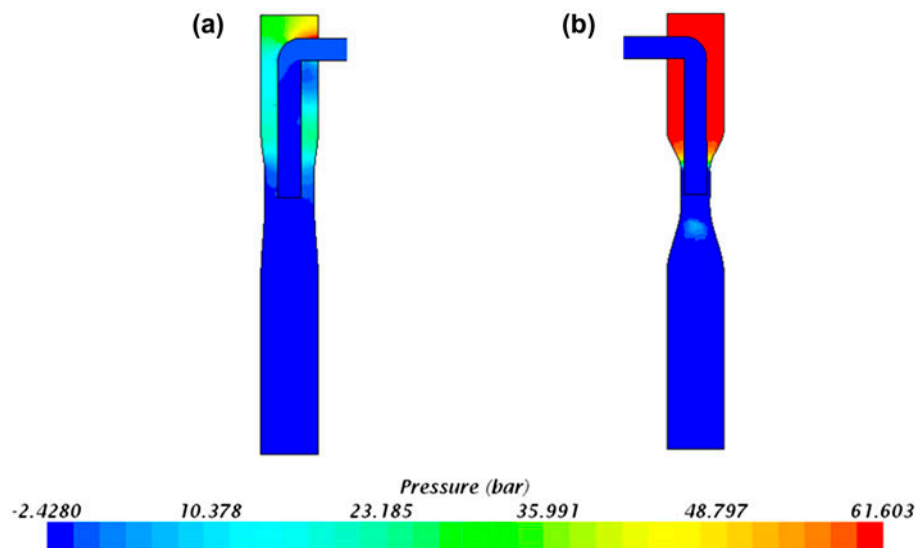
Fig. 6. Pressure profile inside the aspirator for: (a) $A_r = 0.6$; and (b) $A_r = 0.1$.

Similar trends can be observed in Fig. 7(B) and (C) for n_{sheets} values of 10 and 100, respectively. It is observed that increasing the number of membrane sheets in the VMD module (n_{sheets}) reduces the minimum total specific pumping power requirements of the system.

Based on multiple model fits, similar to those shown in Figs. 7 and 8(A) is created which shows the minimum total specific pumping power requirements of the system as a function of n_{sheets}, at the respective optimum m_{feed} for each case and at vacuum pressure of 17 kPa. A general reduction in specific total pumping power is observed as n_{sheets} increases. However, this reduction becomes asymptotic at a specific pump power of about 20 kWh h/m^3 as n_{sheets} approaches 100.

3.2.3. Aspirator vacuum pressure

To investigate the effect of vacuum pressure on the system's pumping power requirements, the above procedure was repeated for a vacuum pressure of 55 kPa. Fig. 8(B) shows the specific and total pumping power as a function of number of membrane sheets in the VMD module at a vacuum pressure of 55 kPa. From Fig. 8(B), it can be seen that, for a given number of membrane sheets, the total pumping power required for the optimized VMD system operating at 55 kPa, vacuum pressure is more than double that of the VMD system at 17 kPa. The pumping power requirement of the aspirator generally increases as the vacuum pressure is decreased, simply because the pump is required to evacuate more gas molecules to

attain a lower pressure. However, at the same time, the higher pressure of the system results in less permeate flow, resulting in the net increase in specific pumping energy. Like at 17 kPa, the specific power curve at 55 kPa is also asymptotic, but at a specific pump power of about 35 kW h/m^3.

4. System energy efficiency

Although relatively high values of specific pump power for the optimized systems were obtained in this study, it is noteworthy that our analyses so far are based on an aspirator contraction area of $A_r = 0.1$. As we have shown in Fig. 5, reducing A_r would reduce the specific pumping power requirement of the system. However, lower contraction ratios will also make the system more prone to cavitation. Clearly, the practicality of using the aspirator as a vacuum generator for the VMD system depends strongly on the user's ability to minimize cavitation and noise in the aspirator's throat, especially at very low aspirator contraction ratios. If that can be achieved, the specific pumping power can even be further reduced.

The thermal energy input to the VMD system to raise the top feed temperature up to 85°C is at least an order of magnitude higher than the electric pumping power requirement discussed in the study. Often, MD systems are advocated in such cases where they can make use of waste heat from industrial processes or renewable energy sources, such as solar or geothermal energy. Even in these cases, it is important to understand and improve the energy efficiency, in the form
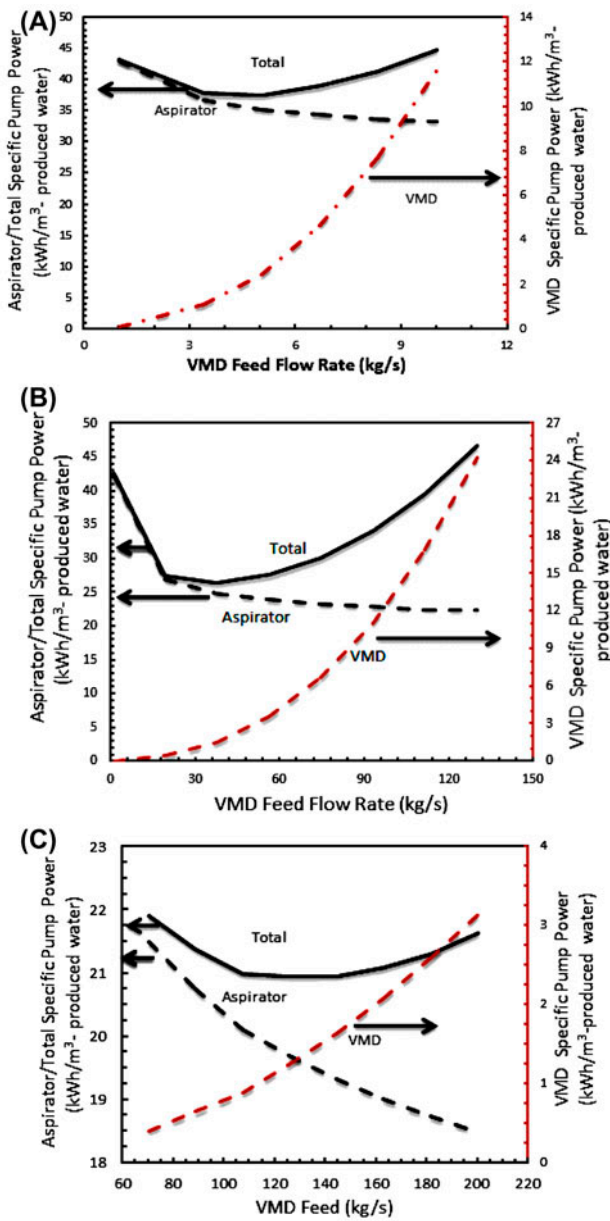
Fig. 7. Specific pumping power variation with m_{feed} at 17 kPa operation pressure (56.6°C saturation temperature) and an aspirator A_r of 0.1 for: (A) single sheet VMD; (B) 10 sheet VMD; and (C) 100 sheet VMD. "Total power" on the y-axis refers to the summation of feed pumping power in the MD system and pure water pumping power in the aspirator loop. The "VMD specific pump power" refers to the feed pumping power in the VMD system on A.

Fig. 8. Minimum total specific pumping power as a function of number of membrane sheets in the VMD module at the m_{feed} leading to minimum power consumption in each respective case: at 17 kPa vacuum pressure, 56.6°C saturation temperature (above); and at 55 kPa, 83.7°C saturation temperature (below). "Total pumping power" on the y-axis refers to the summation of feed pump power in the VMD system and water pump power in the aspirator loop.

of gained output ratio (GOR) of the process, in order to reduce the cost of pure water produced. This is because capital cost is associated with bringing energy into the s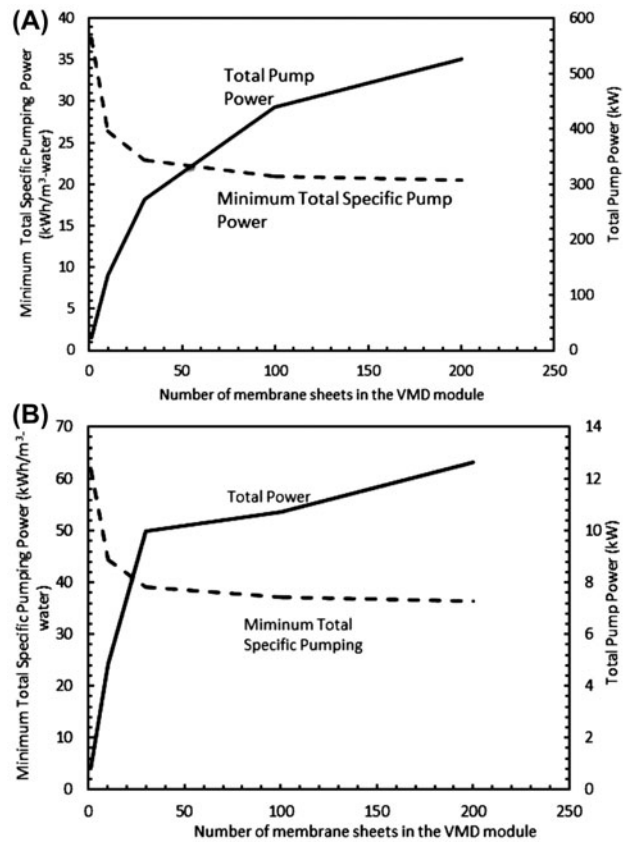ystem, for example, in the form of some area of solar collectors, and this cost generally increases with the amount of energy to be transferred. The GOR for an MD system is defined as:

$$\text{GOR} = \frac{\dot{m}_p h_{fg}}{\dot{Q}_{in}} \tag{18}$$

where $\dot{m}_p$ is the rate of pure water production in kg/s, h_{fg} is the enthalpy of vaporization in J/kg, and $\dot{Q}_{in}$ is the heat supplied to the feed stream in the heater in W. A GOR of 1 corresponds to a specific thermal energy consumption of about 678.3 kW h/m³ (with $h_{fg} = 2,441.68$ kJ/kg and water density = 1,000 kg/m³). A higher GOR value corresponds to lower specific thermal energy consumption.

At the optimal flow rate for a given number of sheets, the system in Fig. 9 could have a GOR as low as 0.02 when the vacuum pressure is 55 kPa and recovery ratio without recirculation is low (0.23%). However, when the vacuum pressure is 5 kPa, the GOR can be as high as 0.7, and the recovery ratio would also be higher (7.88%). The difference in GOR is a result of the increase in recovery ratio at low vacuum pressure, where more pure water is produced for the same heat input. At low recovery, in the 55 kPa cases, the brine is rejected from the system very close to the input temperature of 85°C. Since this energy is wasted, the GOR is relatively low. On the other hand, at higher recovery ratios, the brine is rejected at lower temperatures and hence energy is used more effectively.

The other source of energy recovery is from the low-pressure pure water vapor. The condensation energy of this pure vapor stream can be used to preheat the feed. In the case of the aspirator, due to the relatively low permeate mass flow compared to the mass flow rate of water circulated to generate vacuum in the aspirator loop, the temperature rise caused when the permeate condenses into the aspirator fluid is observed to be inconsequential (see Fig. 10). As a result, condensation energy recovery from the

aspirator liquid is difficult. A solution to this problem is to add an additional condenser before the vapor reaches the aspirator system as shown in Fig. 9. In this case, permeate in the form of liquid water with some amount of vapor and non-condensable gasses would reach the aspirator loop, and the aspirator might need to be correspondingly redesigned as the volume flow rate into the system could be lower.

The extent of condensation is a function of the vapor pressure. The vapor pressure sets the condensation temperature within the vapor channel. If the vapor pressure is low, then the entire vapor volume may not condense since it cannot transfer enough heat into the feed stream due to an unfavorable or small temperature difference available. At the same time, low pressure on the permeate side is necessary for achieving high flux.

On the other hand, energy efficiency can also be improved by recovering energy from the brine discharge. Fig. 9 shows a heat exchanger (regenerator) being used to preheat the feed before it passes into the main heater. Instead, part of the brine water can also be recirculated with additional make up feed water mixed with it. Such a design would be thermodynamically similar to using a regenerator with low terminal temperature difference, except that the feed
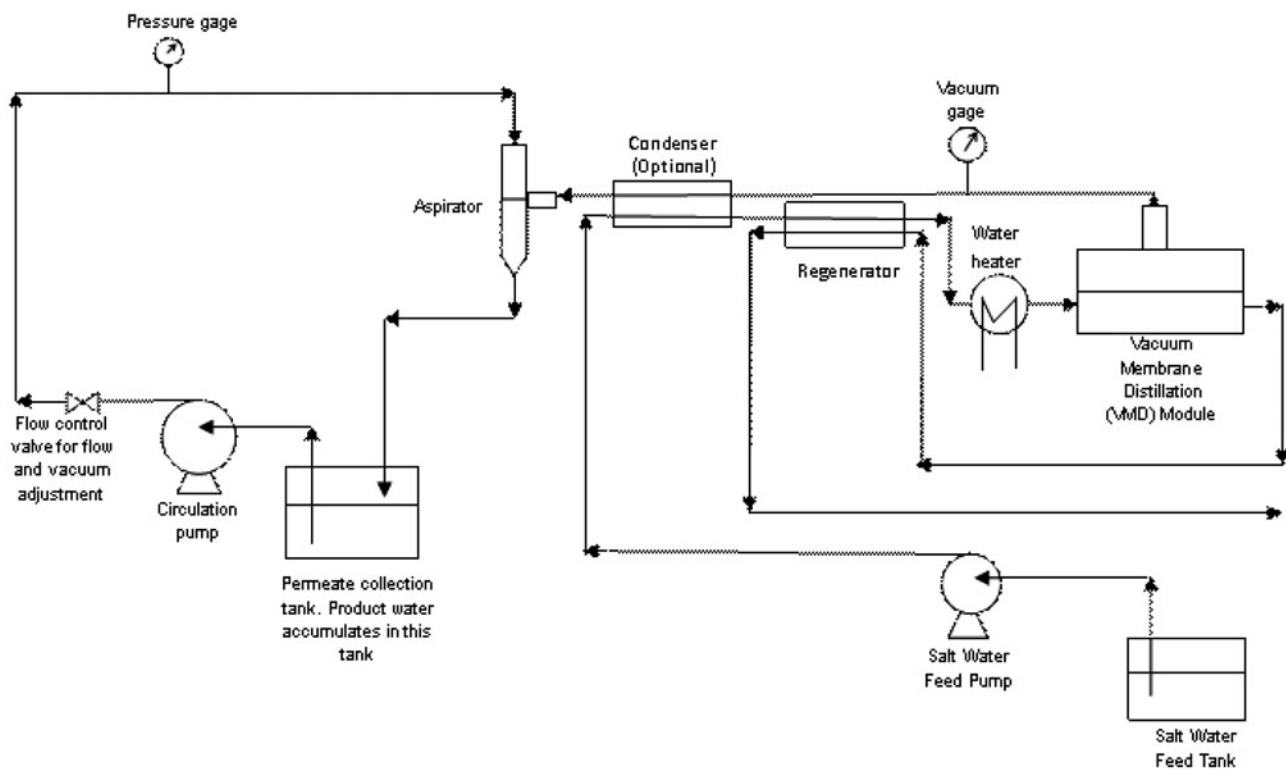

Fig. 9. Aspirator–VMD system with energy recovery devices including permeate vapor condenser and brine regenerator.
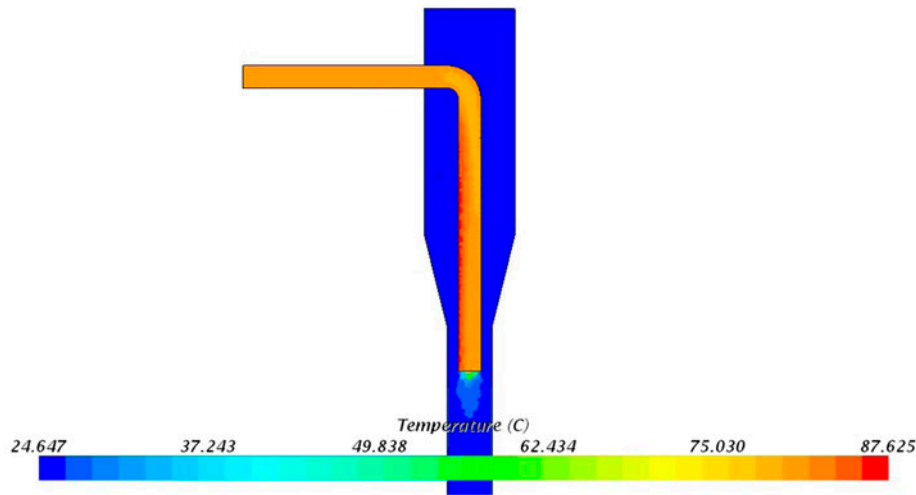
Fig. 10. Temperature profile of the fluid within the aspirator operating at 55 kPa.

salinity would be higher and determined by the ratio of recirculated brine mass flow rate to that of fresh feed water. A combination of these two methods can also be used [12].

Fig. 11 shows the effect of vacuum pressure on GOR under different operating conditions. GOR is lowest when no condenser (C) or regenerator (R) is used. The sizes of the condenser and the regenerator are specified in terms of a pinch point temperature difference (TTD), which is the smallest temperature difference in temperature between the streams. TTD is always greater than 0°C for heat exchangers and a smaller value of TTD corresponds to a larger system size.

There are three sets of curves corresponding to different sizes of regenerator used. In each case, there are two curves corresponding to using or not using a condenser. As expected, adding either of the two components leads to an improvement in GOR. The effect of adding the regenerator is high across a wide range of pressures. On the other hand, the improvement due to the condenser is highest at $P_p \approx 18$ kPa, when the vapor and feed mass flow rates are balanced. At lower pressures, too much vapor is produced, which cannot all condense with the given feed flow rate, which itself gets heated up quicker. In contrast, at higher pressures, a smaller amount of vapor is produced, which cools down to the feed inlet temperature leading to limited preheating.

When a regenerator ($TTD_R = 3$°C) is used, without any condenser, the GOR is higher than in the case of using only a condenser. The difference is not
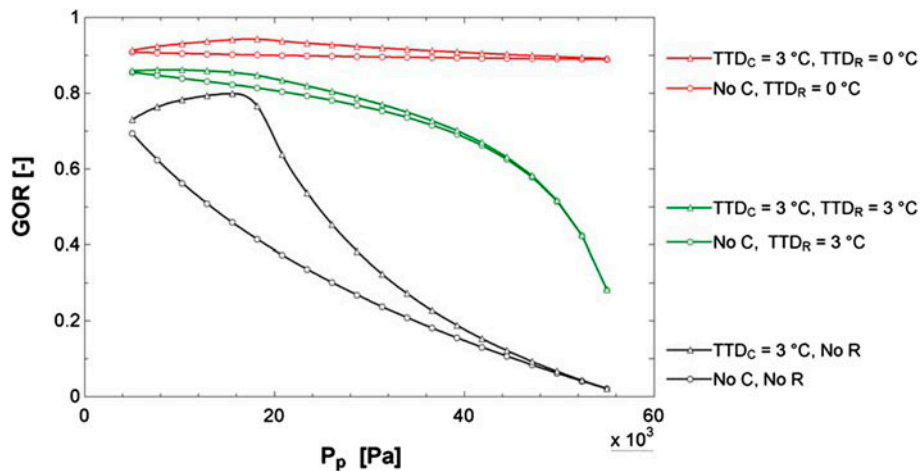

Fig. 11. Effect of regenerator (R) and condenser (C) on GOR of VMD as a function of vacuum pressure.
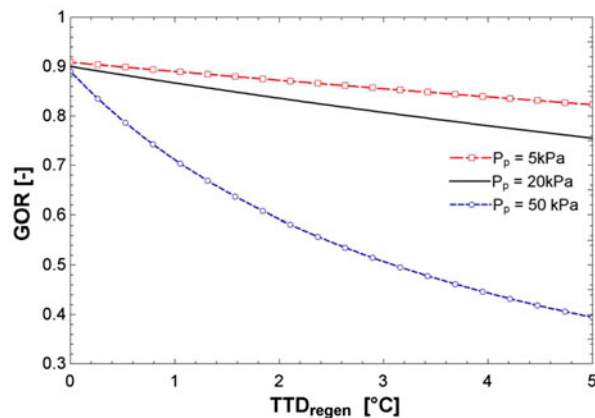
Fig. 12. Effect of regenerator size on GOR at various values of P_p as a function of regenerator terminal temperature difference. No condenser is used.

significant close to the point of balanced operation of the condenser, whereas the improvement with only the regenerator is higher at both higher and lower pressures. The advantage of using a condenser in addition to the regenerator is much smaller, compared to the effect of a condenser when no regenerator is used.

Finally, setting the terminal temperature difference equal to 0°C in the regenerator helps simulate the best case performance in the case of brine recirculation, ignoring the effects of salinity [12]. Under this condition, assuming no heat loses as in the other cases, the GOR achievable is almost independent of the permeate pressure. The effect of adding a condenser is small, just as in the case of $TTD_R = 3$°C.

Fig. 12 shows the effect of regenerator size on GOR at different values of permeate pressure. In all cases, the GOR of a single-stage VMD system is limited to a value less than 1.

5. Comparison with conventional VMD systems

In the case of a conventional VMD system, at lower pressures, additional cooling water is required in addition to the feed flow rate to achieve complete condensation of the vapor. This is possible only if the saturation temperature of the vapor is higher than that of the incoming seawater (i.e. $P_p > 5$ kPa, if feed enters at ambient temperature). If the vapor pressure is lower than even this limit, additional cooling systems will be necessary to condense the pure water.

Vacuum pumps often cannot handle moisture in the air. As a result, an additional moisture trap is used to condense the vapor that remains after the condenser in these conventional designs. A liquid pump

is also required in this system to pump out the condensed low-pressure liquid pure water up to atmospheric pressure. While the energy consumption of this pump is not very high, this results in additional capital expenditure.

If initial evacuation of the module is ignored, the power required to maintain the vacuum is related to total volume flow rate of permeate and non-condensable gasses that need to be removed from the system. In this context, the vacuum pump power is given by:

$$P_{vac} = \frac{\dot{Q}_v \Delta P}{\eta_p} \tag{19}$$

where $\dot{Q}_v$ is the volume flow rate, ΔP is the change in pressure, and η_p is the pump's efficiency. If complete condensation is achieved, only the dissolved gasses will have to be pumped out by the vacuum pump. For $P_p = 5$ kPa and $\eta_p = 70\%$, the specific energy consumption of the ideal vacuum pump and liquid pump system is about 0.04 kW h/m^3 if only the non-condensable gasses (0.0153 g/kg-feed) need to be pumped by the vacuum pump and complete vapor condensation is achieved. As discussed previously, using the feed flow as coolant, only 20% of the vapor can be condensed. Even if additional cooling water is used, complete condensation is not achieved. For example, if five times the feed water flow rate is used, about 55% of the vapor is condensed, whereas if eight times the feed water flow is used as coolant, about 84% of the vapor is condensed, if the condenser TTD is fixed at 3°C. The amount of additional feed water required for complete condensation is illustrated in Fig. 13 as a function of the vacuum pressure, assuming a TTD of 3°C.
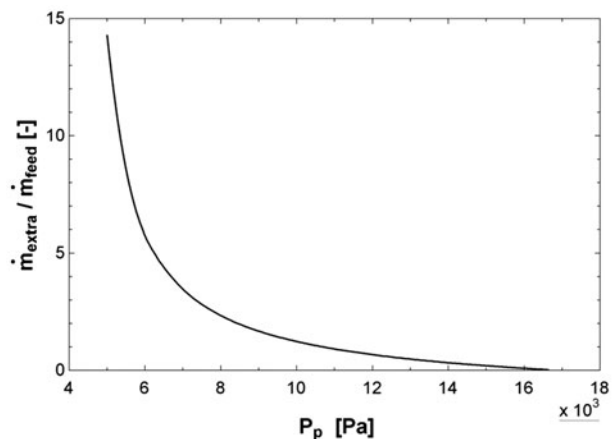

Fig. 13. Additional water required for complete condensation as a function of vacuum pressure ($TTD_c = 3$°C).

In order to account for incomplete condensation and other air leakage effects within the vacuum system, we evaluate the pumping power requirement if the flow rate through the pump is higher. If 4% of the vapor passes to the vacuum pump, the conventional systems theoretical power consumption would increase to about 1.37 kW h/m^3. However, if 60% of the vapor passes to the vacuum pump, this energy consumption would increase to 16.02 kW h/m^3. This pump's specific power is comparable to that of the aspirator's pump, with a VMD system of 30 membrane sheets.

The aspirator system has a significant advantage since even if an additional condenser is used; complete condensation is not a necessity. The capital expenditure for condensers, vacuum pumps, and liquid pumps are eliminated in favor of a cheaper adjustable system with lower maintenance requirements. On the other hand, as a pump is required to convey the aspirator's fluid, the cost of adapting the aspirator is not insignificant.

As noted previously, the GOR of single-stage VMD systems is restricted to a value less than 1 irrespective of the nature of energy recovery used. This is the motivation behind the design of multi-staged MD systems. These can either be designed similar to multi-effect distillation systems [22] or multi-staged flash (MSF) systems [23]. In the case of MSF type multi-staged VMD, condensers would be used between stages to recover energy from the pure vapor condensation to preheat water. In the case of the MED type system, the condensation would be used to heat feed in a subsequent stage. In both these cases, a vacuum still needs to be actively maintained, which can be achieved using the proposed aspirator system. The relative advantage of the aspirator in these cases needs to be investigated more thoroughly.

6. Conclusions

The concept of using an aspirator as the vacuum generator for a VMD system has been introduced and analyzed. Validation of the proposed concept has been carried out via CFD. A coupled flow analysis of the aspirator, a membrane desalination unit, and auxiliary devices has been performed for optimization purposes. A lower aspirator contraction ratio is found to lead to a lower aspirator pump power. However, the problem of cavitation and noise is more prevalent in the lower contraction ratio design. The total specific pumping power (VMD feed pump plus aspirator water pump) can reach approximately 20 kW h/m^3, using up to 100 membrane sheets in the VMD module. However, increasing the number of sheets above 30

does not yield any significant reduction in specific pumping power. As this analysis is based on an aspirator contraction ratio of 0.1, which may result in cavitation and noise, further studies are recommended to address this potential issue. If cavitation can be suppressed, the specific pump power of the system may be further lowered by further reduction of the contraction ratio. The proposed aspirator–VMD system achieves energy efficiencies similar to that of conventional single-stage VMD systems while eliminating many of the concerns associated with the conventional design of using a condenser and a vacuum pump, such as incomplete vapor condensation, continuity of vacuum pump operation, and the risk of water vapor damage to the pump. The proposed system may also be coupled with multi-stage VMD systems that have higher GOR. The total pumping power required by a vacuum pump in a conventional single-stage VMD device during steady-state operation is likely to be lower than that used by the aspirator system, although in cases where complete condensation is not achieved and part of the vapor is pumped out by the vacuum pump, the power requirement may be of comparable magnitude to that of the aspirator system.

Nomenclature

d_1	—	aspirator's entrance cylinder diameter (m)
L	—	aspirator's entrance cylinder length (m)
d_2	—	aspirator's throat's diameter (m)
l	—	aspirator's throat length (m)
d_i	—	needle's diameter (m)
m_{feed}	—	VMD feed flow (kg/s)
n_{sheets}	—	number of membrane sheets
$Power_{feed}$	—	power requirement of the VMD feed pump (W)
$Power_{asp}$	—	power requirement of aspirator feed pump (W)
P	—	pressure (Pa)
C_d	—	pump's discharge coefficient
ρ	—	density (kg/m^3)
v	—	velocity (m/s)
g	—	gravitational constant (m/s^2)

z	—	elevation (m)
A	—	area (m^2)
m_p	—	permeate mass flow (kg/s)
A_r	—	aspirator's contraction area (m)
ϵ_p	—	pump efficiency
vol_p	—	volume flow rate of permeate (m^3/s)
Q	—	heat flow through membrane (W)
h_w	—	heat transfer coefficient (W/m^2 K)
T_b	—	bulk fluid temperature (K)
T_m	—	membrane surface temperature (K)
Nu	—	Nusselt number
f	—	Friction coefficient
Re	—	Reynolds number
Pr	—	Prandtl number
k	—	thermal conductivity (W/m K)
A_c	—	piping wetted area (m)
h_{pm}	—	specific enthalpy of vapor at the permeate side (J/kg)
h_b	—	specific enthalpy of feed flow (J/kg)
J	—	mass flux through the membrane (kg/s)
h_{fg}	—	enthalpy of vaporization (J/kg)
η_p	—	pump efficiency (%)
AGMD	—	air gap membrane distillation
CFD	—	computational fluid mechanics
DCMD	—	direct contact membrane distillation
EES	—	Engineering Equation Solver
GOR	—	gained output ratio
MD	—	membrane distillation
RO	—	reverse osmosis
SGMD	—	sweeping gas membrane distillation
VMD	—	vacuum membrane distillation

References

[1] M. Khayet, T. Matsuura, Membrane Distillation: Principles and Applications, Elsevier, Oxford, 2011.

[2] S.S. Köseoglu, D.E. Engelgau, Membrane applications and research in the edible oil industry: An assessment, J. Am. Oil Chem. Soc. 67 (1990) 239–249.

[3] D. Winter, J. Koschikowski, M. Wieghaus, Desalination using membrane distillation: Experimental studies on full scale spiral wound modules, J. Membr. Sci. 375 (2011) 104–112.

[4] J. Koschikowski, M. Wieghaus, M. Rommel, Solar thermal-driven desalination plants based on membrane distillation, Desalination 156 (2003) 295–304.

[5] S.A. Kalogirou, Seawater desalination using renewable energy sources, Prog. Energy Combust. Sci. 31 (2005) 242–281.

[6] F. Banat, N. Jwaied, Economic evaluation of desalination by small-scale autonomous solar-powered membrane distillation units, Desalination 220 (2008) 566–573.

[7] R.B. Saffarini, E.K. Summers, H.A. Arafat, J.H. Lienhard V, Economic evaluation of stand-alone solar powered membrane distillation systems, Desalination 299 (2012) 55–62.

[8] R.B. Saffarini, E.K. Summers, H.A. Arafat, J.H. Lienhard V, Technical evaluation of stand-alone solar powered membrane distillation systems, Desalination 286 (2012) 332–341.

[9] K.W. Lawson, D.R. Lloyd, Membrane distillation. I. Module design and performance evaluation using vacuum membrane distillation, J. Membr. Sci. 120 (1996) 111–121.

[10] Internatinal Standards Organization (ISO), ISO-5167: Measurement of Fluid Flow by Means of Pressure Differential Devices Inserted in Circular CROSS sections. Part 1–4, ISO, 2003.

[11] N. Marquardt, Introduction to the Principles of Vacuum, in CERN European Organization for Nuclear Research Reports, Dortmund, 1999.

[12] E.K. Summers, H.A. Arafat, J.H. Lienhard, Energy efficiency comparison of single-stage membrane distillation (MD) desalination cycles in different configurations, Desalination 290 (2012) 54–66.

[13] M.I. Ali, E.K. Summers, H.A. Arafat, J.H. Lienhard V, Effects of membrane properties on water production cost in small scale membrane distillation systems, Desalination 306 (2012) 60–71.

[14] Star CCM+, CD Adpaco, Available from: <http://www.cd-adapco.com/>.

[15] S. Dushman, M. Lafferty, *Scientific Foundations of Vacuum Technique*, Wiley, New York, NY, 1962, p. 99.

[16] L. Rayleigh, On the pressure developed in a liquid during the collapse of a spherical cavity, Philos. Mag. 34 (1917) 94–98.

[17] M. Plesset, The dynamics of cavitation bubbles, ASME J. Appl. Mech. 16 (1947) 228–231.

[18] J.I. Mengual, M. Khayet, M.P. Godino, Heat and mass transfer in vacuum membrane distillation, Int. J. Heat Mass Transfer 47 (2004) 865–875.

[19] K.W. Lawson, D.R. Lloyd, Membrane distillation, J. Membr. Sci. 124 (1997) 1–25.

[20] R.W. Schofield, A.G. Fane, C. Fell, Heat and mass transfer in membrane distillation, J. Membr. Sci. 33 (1987) 299–313.

[21] V. Gnielinski, New equations for heat and mass-transfer in turbulent pipe and channel flow, Int. Chem. Eng. 16 (1976) 359–368.

[22] K. Zhao, W. Heinzl, M. Wenzel, S. Büttner, F. Bollen, G. Lange, S. Heinzl, N. Sarda, Experimental study of the memsys vacuum-multi-effect-membrane-distillation (V-MEMD) module, Desalination 323 (2013) 150–160.

[23] H.T. El-Dessouky, H.M. Ettouney, Y. Al-Roumi, Multistage flash desalination: Present and future outlook, Chem. Eng. J. 73 (1999) 173–190.